Submitted to IEEE/RSJ Int. Conf. on Intelligent Robots and Systems. Grenoble, France, Sept. 1997.

On-line Automatic Tipover Prevention for Mobile Manipulators

D. A. Rey dan@cim.mcgill.edu
E. G. Papadopoulos egpapado@cim.mcgill.edu
Department of Mechanical Engineering and Center for Intelligent Machines
McGill University
Montréal, Québec H3A 2A7

Abstract

Mobile manipulators operating in field environments are susceptible to dangerous and costly rollover or tipover instabilities, particularly when operating over uneven terrain or when exerting large forces or moments. By monitoring the static and dynamic tipover stability margins of a mobile manipulator it is possible to predict such tipovers and take appropriate actions to prevent the tipover from occurring. This paper describes a scheme for automatic tipover prediction, and prevention, which uses the static and dynamic Force–Angle measures of tipover stability margin. Time-until-tipover prediction is accomplished using estimated gradients of the tipover stability margins, and prevention is accomplished using a combination of the manipulator and platform actuators. Simulation results demonstrate the efficiency and promise of the proposed scheme for automatic tipover prevention.

1 Introduction

Mobile machines equipped with manipulator arms and controlled by on-board human operators are commonplace systems in the construction, mining, and forestry industries, see for example Fig. 1. When these systems exert large forces, move heavy payloads, or operate over very uneven or sloped terrain, tipover instabilities may occur which endanger the operator, reduce productivity, and risk damaging the machine. Teleoperated or fully autonomous mobile manipulators operating in field environments (as proposed by the nuclear, military and aerospace industries) are also susceptible to such mission critical tipovers. With the introduction of computer control (i.e. a supervisory control system) the safety, productivity and lifetime of these mobile manipulators could be improved by automatic prediction and prevention of a tipover instability. In order to accomplish this, appropriate measures of the tipover stability margin must be used and appropriate responses to an impending tipover executed without delay.

Work by the vehicular research community has focused on characterizing the lateral rollover propensity of a vehicle and on providing physical safety barriers to protect an operator in the event of a tipover [1, 2].

Attempts by the robotics research community to solve the motion planning problem for mobile manipulators travelling over sloped terrain, or exerting large forces or moments on the environment, gave rise to various stability constraint definitions [3, 4]. Several researchers examined more directly the question of how one should define the instantaneous stability margin for a mobile manipulator [5, 6, 7, 8, 9]. These works however do not address the questions of how to automatically *predict* and *prevent* tipover instabilities.

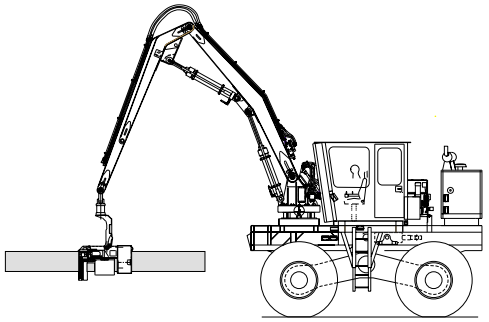

Fig. 1: **Example mobile manipulator.**

This work describes the two types of tipover instability which may occur for mobile manipulators operating over uneven terrain: tipover in the absence of destabilizing inertia forces (static instability), and tipover in the presence of destabilizing inertia forces (dynamic instability). The simultaneous use of two tipover stability margin measures, static and dynamic, are thus prescribed herein for automatic tipover prediction and prevention. This work makes use of the dynamic Force–Angle stability margin measure presented in [10], and introduces a static version of the latter. A simple and effective tipover prediction method is described, as well as an algorithm for triggering a tipover prevention response. Various tipover prevention actions approaches are then described and their performances compared for the case of a simulated forestry vehicle executing an unstable manoeuvre.

2 Tipover prediction

To prevent a tipover instability it is first necessary to *predict* a possible onset of tipover. This can be accomplished by monitoring the tipover stability margin of a system [10], estimating its gradient, and then computing the predicted time-until-tipover (i.e. the time

remaining until tipover if the gradient were to remain unchanged.) Note that the measure used here must be a measure of the stability *margin* and must evolve as the system configuration evolves.

2.1 Force–Angle tipover stability margin measure

The tipover stability margin measure selected for use in this work was the Force–Angle stability margin measure given its sensitivity to vehicle center-of-mass height (topheaviness), its ease of implementation, and its applicability to systems operating over arbitrarily uneven terrain and subject to inertial and external forces [10]. The simple nature of the Force–Angle measure and the fact that it does not require any integration are other important advantages. For completeness we summarize here the nature of the Force–Angle tipover stability margin measure and present the key equations of [10].

The fundamental premise of the Force–Angle measure is that the tipover stability margin of a mobile manipulator can be compactly described as the minimum of the angles between the resultant force $\mathbf{f}_r$, acting on the vehicle center-of-mass, and the tipover axis normals $\mathbf{l}_i$ directed from the center-of-mass. The result is then weighted by the resultant force magnitude for heaviness sensitivity. For a system with n tipover axes the Force–Angle measure is thus given by

$$\alpha = \min\left(\theta_i\right) \|\mathbf{f}_r\| \qquad i = \{1, \ldots, n\} \tag{1}$$

where the angles θ_i are given by

$$\theta_i = \sigma_i \cos^{-1}\left(\hat{\mathbf{f}}_i^* \cdot \hat{\mathbf{l}}_i\right) \qquad i = \{1, \ldots, n\} \tag{2}$$

See for example the planar system of Fig. 2 or the three dimensional system of Fig. 3. It can be seen that the tipover stability margin, α, appropriately goes to zero when the magnitude of any of the angles (θ_i) or the force ($\mathbf{f}_r$) goes to zero. A singular condition exists when the vehicle center-of-mass lies on, or near, a tipover axis. However, it is reasonable to assume that this is not the case as the vehicle's fundamental design would be statically unstable.

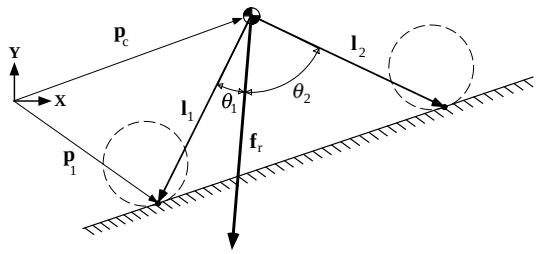

Fig. 2: **Planar Force–Angle stability measure.**

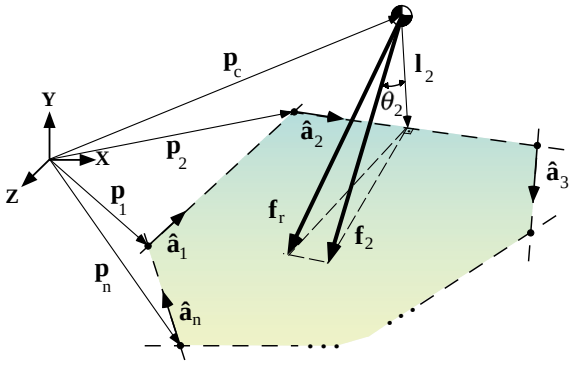

Fig. 3: **3D Force–Angle stability measure.**

For each tipover axis $\mathbf{a}_i$, the effective net tipover force $\mathbf{f}_i^*$ is found by considering only that component of $\mathbf{f}_r$ orthogonal to $\mathbf{a}_i$, and by adding an equivalent force couple component $\mathbf{f}_{n_i}$ to replace any angular loads acting about the vehicle center-of-mass, i.e.

$$\mathbf{f}_i^* = \left(\mathbf{1} - \hat{\mathbf{a}}_i \hat{\mathbf{a}}_i^T\right) \mathbf{f}_r + \mathbf{f}_{n_i} \tag{3}$$

with

$$\mathbf{f}_{n_i} = \frac{\hat{\mathbf{l}}_i \times \mathbf{n}_i}{\|\mathbf{l}_i\|} \tag{4}$$

(Note that boldface is used herein to represent a *column* vector.) The appropriate sign of θ_i is determined by establishing whether or not the effective net tipover force $\mathbf{f}_i^*$ is directed inside or outside the support pattern, i.e.

$$\sigma_i = \begin{cases} +1 & \left(\hat{\mathbf{f}}_i^* \times \hat{\mathbf{l}}_i\right) \cdot \hat{\mathbf{a}}_i > 0 \\ -1 & \text{otherwise} \end{cases} \qquad i = \{1, \ldots, n\} \tag{5}$$

Dynamic measure. The resultant force $\mathbf{f}_r$ acting on the vehicle center-of-mass which would participate in a tipover instability is given by

$$\mathbf{f}_r\big|_{\text{dyn}} \triangleq \Sigma\, \mathbf{f}_{\text{grav}} + \Sigma\, \mathbf{f}_{\text{manip}} + \Sigma\, \mathbf{f}_{\text{dist}} - \Sigma\, \mathbf{f}_{\text{inertial}} \tag{6}$$

$$= -\Sigma\, \mathbf{f}_{\text{support}} \tag{7}$$

where $\mathbf{f}_{\text{grav}}$ are the gravitational loads, $\mathbf{f}_{\text{manip}}$ are the loads transmitted by the manipulator to the vehicle body (due to manipulator dynamics, end-effector loading, and end-effector reaction forces), $\mathbf{f}_{\text{inertial}}$ are the inertial forces, $\mathbf{f}_{\text{dist}}$ are any external disturbance forces acting directly on the vehicle (e.g. forces due to a trailer implement) and, $\mathbf{f}_{\text{support}}$ are the reaction forces of the vehicle support system.

The effective net tipover moment $\mathbf{n}_i$ is given by

$$\mathbf{n}_i\big|_{\text{dyn}} = \left(\hat{\mathbf{a}}_i \hat{\mathbf{a}}_i^T\right)\left(\Sigma\, \mathbf{n}_{\text{manip}} + \Sigma\, \mathbf{n}_{\text{dist}} - \Sigma\, \mathbf{n}_{\text{inertial}}\right) \tag{8}$$

Using $\mathbf{n}_i|_{\text{dyn}}$ in eq. (4) and $\mathbf{f}_r|_{\text{dyn}}$ in eqs. (1) and (3) yields the *dynamic* stability margin $\alpha|_{\text{dyn}}$.

Static measure. In computing the *static* Force–Angle stability margin measure we assume that the only loads acting on the system are static loads. Thus, all expressions are as before but with all velocities and accelerations set to zero. Generally, this will yield

$$\mathbf{f}_r\big|_{\text{stat}} = \Sigma\, \mathbf{f}_{\text{grav}} + \Sigma\, \mathbf{f}_{\text{manip}} \tag{9}$$

and

$$\mathbf{n}_i\big|_{\text{stat}} = \left(\hat{\mathbf{a}}_i \hat{\mathbf{a}}_i^T\right) \Sigma\, \mathbf{n}_{\text{manip}} \tag{10}$$

Using $\mathbf{n}_i|_{\text{stat}}$ in eq. (4) and $\mathbf{f}_r|_{\text{stat}}$ in eqs. (1) and (3) yields the static stability margin $\alpha|_{\text{stat}}$.

Normalisation. For ease of interpretation and proper numerical conditioning we normalise each of these α by their nominal values, i.e.

$$\hat{\alpha} = \frac{\alpha}{\alpha_{\text{nom}}} \tag{11}$$

where α_{nom} is the nominal value of α for the system in its home configuration on level ground. Both the static and dynamic $\hat{\alpha}$ are thus equal to 1 for the nominal configuration system on a level surface.

2.2 Time-until-tipover

In order to determine when to trigger an automatic tipover prevention response it is best to augment our knowledge of the system's present stability state, $\alpha|_{\text{dyn}}$ and $\alpha|_{\text{stat}}$, by also tracking their time rate of change: $\dot{\alpha}|_{\text{dyn}}$ and $\dot{\alpha}|_{\text{stat}}$. Various methods can be used to compute these gradients. A closed-form least squares approach was found to yield smooth and rapid slope estimates.

A single measure which combines both stability margin information and stability margin gradient information, is the predicted *time-until-tipover*. Since a tipover is predicted when extrapolation of α yields a zero crossing we have simply

$$t_{\text{tip}} = -\hat{\alpha} \,/\, \dot{\hat{\alpha}} \tag{12}$$

Two time-until-tipover predictions are simultaneously computed, one for each of the static and dynamic $\hat{\alpha}$. These instantaneous measures change at every time step with both $\hat{\alpha}$ and $\dot{\hat{\alpha}}$.

3 Tipover prevention

In order to avoid unnecessary execution of a tipover prevention response it is required to ignore predictions of imminent tipover which are of brief transient (and not truly indicative of a danger to the system.) This is accomplished by only initiating a response if the predicted time-until-tipover remains below some threshold for a given period of time, i.e. the tipover prediction is persistent. The proposed triggering algorithm consists here of a running maximum over k points as follows:

`if`

$$\max\left(t_{\text{tip}_{n-k}},\ t_{\text{tip}_{n-k+1}},\ \ldots,\ t_{\text{tip}_n}\right) < t_{\text{threshold}}$$

`then`

perform tipover prevention response

where $t_{\text{threshold}}$ is set much smaller than the system fundamental period.

3.1 Tipover prevention response

The Force–Angle stability margin equation, eq. (1), reveals the two possible elements of a tipover prevention action: a geometric correction (where one attempts to increase $\min(\theta_i)$), and a loading correction (where one attempts to increase $\mathbf{f}_r$). This work focuses on the more practical approach of increasing $\min(\theta_i)$.

Eq. (2) reveals that $\min(\theta_i)$ can be increased by altering the direction of either $\mathbf{f}_i^*$ or $\hat{\mathbf{l}}_i$ in order to increase their angular separation. A variety of techniques are possible to achieve this goal. One geometric technique is to relocate the vehicle center-of-mass position $\mathbf{p}_c$, with respect to the tipover axis $\mathbf{a}_i$. For a legged system this can be accomplished by changing the system footing. However, for wheeled or tracked systems, this is not a valid option without special actuators. A second technique consists of altering $\mathbf{f}_i^*$ by using the manipulator and/or the vehicle mobility actuators (i.e. wheels, tracks or legs). Using this technique, an effective response to a potential static instability ($\alpha|_{\text{stat}} \to 0$) has been determined to be the following combined use of both the manipulator and the vehicle mobility actuators:

1) *return the manipulator to its inertial home configuration (where the inertial home configuration is assumed to be that posture for which the manipulator exerts a negligible moment on the vehicle base), and*

2) *simultaneously use the vehicle mobility actuators to compensate for any temporarily destabilizing dynamic moments at the manipulator base.*

The first action redirects $\mathbf{f}_i^*$ away from the tipover axis and toward the interior of the support polygon, while the second action stabilizes the vehicle throughout the recovery motion. In fact, the second action can be considered and implemented as a feedback law where the manipulator base joint destabilizing moment is computed and used to derive the vehicle mobility actuator commands. The stability of this manoeuvre throughout its execution can be fully guaranteed if the vehicle wheels, tracks or legs are able to exert the required compensation loads in both direction and magnitude.

Arm trajectory generation. While a variety of trajectories are possible for ensuring a smooth return of the manipulator to its inertial home configuration,

it was found that satisfactory results are obtained by using a quintic polynomial trajectory subject to the 3 initial boundary conditions of present joint angle, velocity and acceleration, and the 3 final boundary conditions of joint home angle, zero final velocity and zero final acceleration. The closed-form solution can be used for real-time joint trajectory generation when a tipover prevention response is initiated. The duration of the motion is arbitrary, yet it should be chosen sufficiently large to prevent saturation of the actuators under worst-case conditions.

Base joint feedback. To compensate for any destabilizing moments on the vehicle base which may arise as a result of retracting the manipulator, we first compute the disturbing base joint moment on the vehicle, $\mathbf{n}_b$, by subtracting the nominal gravity feedforward torque applied to the manipulator base joint, $\boldsymbol{\tau}_{\mathrm{ff}_1}$, from the net torque applied to the manipulator by the base joint actuator $\boldsymbol{\tau}_{m_1}$, i.e.

$$\mathbf{n}_b = -\left(\boldsymbol{\tau}_{m_1} - \boldsymbol{\tau}_{\mathrm{ff}_1}\right) \tag{13}$$

The component of $\mathbf{n}_b$ which lies along the current predicted tipover axis $\mathbf{a}_i$ is the destabilizing moment which we seek to compensate using an applied torque $\boldsymbol{\tau}_w$ to the vehicle wheels, legs, or tracks. Thus, the applied torque $\boldsymbol{\tau}_w$ is chosen so that its component along $\mathbf{a}_i$ is as equal and opposite to the destablizing component of the $\mathbf{n}_b$ moment as possible, i.e. choose $\boldsymbol{\tau}_w$ so as to

$$\min \left\| \left(\boldsymbol{\tau}_w - \mathbf{n}_b\right)^T \mathbf{a}_i \right\| \tag{14}$$

Solution of eq. (14) can be accomplished in real-time by determining the appropriate mapping from $\mathbf{n}_b$ to $\boldsymbol{\tau}_w$ which minimizes the given norm, as a function of the vehicle mobility architecture and state. Once this mapping is established in closed-form for a given vehicle, it can then be used in a closed-loop feedback law to generate the desired wheel, track or leg commands.

4 Example

Automatic tipover prediction and prevention using the Force–Angle stability margin measure was implemented in a planar simulation of a mobile manipulator with fundamental characteristics similar to that of the forestry vehicle of Fig. 1. The five body system consists of a principal vehicle body, a pair of pneumatic tires, a two degree-of-freedom revolute joint manipulator with rigid links, and a rigidly attached end-effector or tool. The longitudinal plane model captures inertial effects, external loading effects, tire slip and compliance. Manipulator masses are assumed lumped at the joints. Key system parameters are listed in Table 1.

The seven generalized coordinates of the system are the three vehicle inertial pose coordinates (i.e vehicle center-of-mass position (x_v, y_v), and vehicle pitch angle (θ_z)) the two wheel angular positions, (θ_i), and the two manipulator joint angles, (ϑ_i), so we have

$$\boldsymbol{q} = \left[\, \boldsymbol{q}_v \mid \boldsymbol{q}_w \mid \boldsymbol{q}_m \,\right]^T = \left[\, x_v,\ y_v,\ \theta_z \mid \theta_1,\ \theta_2 \mid \vartheta_1,\ \vartheta_2 \right]^T \tag{15}$$

The system equations of the motion can be shown to be of the form

$$\boldsymbol{I}(\boldsymbol{q})\,\ddot{\boldsymbol{q}} + \mathbf{c}(\boldsymbol{q},\,\dot{\boldsymbol{q}}) + \boldsymbol{\gamma}(\boldsymbol{q}) = \boldsymbol{\tau} + \boldsymbol{\phi}(\boldsymbol{q},\,\dot{\boldsymbol{q}}) \tag{16}$$

where the $\boldsymbol{I}$, $\mathbf{c}$, and $\boldsymbol{\gamma}$ are the inertia, velocity-dependent, and gravity tensors respectively, $\boldsymbol{\tau}$ are the generalized input forces, and $\boldsymbol{\phi}$ are the generalized external loads. The input force vector is of the form,

$$\boldsymbol{\tau} = \left[\, \mathbf{0}^T \mid \boldsymbol{\tau}_w^T \mid \boldsymbol{\tau}_m^T \,\right]^T \tag{17}$$

where both $\boldsymbol{\tau}_w$ and $\boldsymbol{\tau}_m$ are nominally determined using simple PD regulation about a desired vehicle trajectory and desired joint trajectories respectively. The external load vector $\boldsymbol{\phi}$ is given by the sum of the ground forces and moments acting on the system and the prescribed end-effector loads. No other external loads are assumed to be acting on the system. The longitudinal ground forces are determined using a Karnopp slip-stick friction model [11]. The tire model accounts for the special cases of wheel hop or lift-off, locked wheels, backsliding, and reverse direction motion. The normal ground forces are prescribed at each tire contact patch by a first order spring–damper tire compliance model.

Tipover prevention response parameters. For this system it was found heuristically that an approriate trigger time $t_{\mathrm{threshold}}$, was 0.15 seconds until tipover, which is an order of magnitude smaller than the system fundamental period. The duration of the arm retraction motion trajectory was set to 3 seconds.

Unstable sample task. The sample task used here to demonstrate a unstable manoeuvre requiring automatic tipover preventing action has three principal phases: i) the system is initially at rest on a level surface with the manipulator in its home configuration

Table 1: **System parameters**

	mass [kg]	length [m]	mom. of inertia [kgm^2]
vehicle	10,000	–	10,000
link 1	500	3.5	500
link 2	500	3.5	500
tool	1000	–	4000
vehicle c.m. position [m]			$\mathbf{p}_c = [\ 0.00,\ 0,\ \ 0.00]^T$
front wheel hub position [m]			$\mathbf{p}_1 = [\ 1.50,\ 0, -0.25]^T$
rear wheel hub position [m]			$\mathbf{p}_2 = [-0.50,\ 0, -0.25]^T$
manipulator base position [m]			$\mathbf{p}_b = [\ 0.50,\ 0,\ \ 0.00]^T$
undeformed tire radii [m]			$r_{\mathrm{und}} = 0.65$
nomimal joint angles			$\mathbf{q}_{\mathrm{m}} = [\,120^\circ,\ -150^\circ\,]^T$
nominal θ_i (see eq. (2))			$\theta_i = [\,53.0^\circ,\ 45.8^\circ\,]$

holding a heavy object (7500 kg), ii) the manipulator is commanded to reach forward, and iii) a tipover instability occurs after 8.5 seconds unless preventive action is taken.

4.1 Results

Simulation studies demonstrated that when the system is dynamically stabilized (for example by manipulator reaction forces as the arm extends forward) the dynamic stability margin measure fails to detect a potentially precarious static state of the system, i.e. a state which is unstable if the manipulator were to come to a stop (as would occur if the manipulator reached its target or the edge of its workspace.) Thus, when the dynamically stabilizing loads go to zero the stability margin drops very substancially and suddenly, making a safe tipover prevention action very difficult. This problem was solved by simultaneously tracking both the system's static and dynamic stability margins, and computing each of their corresponding time-until-tipover predictions. A tipover prevention response can then be triggered by either measure.

Three case results are presented here to show the effectiveness of the proposed tipover prevention method. The first case is the unstabilized reference case, the second case is the result of attempting stabilization using only the manipulator (i.e. action 1 of section 3.1), and the third case is the fully stabilized case where both the manipulator and vehicle drive wheels are used (i.e. actions 1 and 2 of section 3.1). For each case we present the time histories of the key configuration variables and the static and dynamic Force-Angle stability margin measures.

Figures 4 and 5 show the system evolution for the unstabilized reference case. We see that as the manipulator joint trajectories are followed, tipover occurs at approximately 8.5 seconds. After which the independent PD controllers fail to maintain the desired joint positions.

Figures 6 and 7 show the result of using only the manipulator to attempt to prevent tipover. No drive wheel torques are applied for this case. Since Fig. 7 and Fig. 5 are identical despite the differences in the configuration evolution, we can see clearly that using only the manipulator without exerting any forces on the environment only results in a system configuration change and tipover occurs at the same instant as for the reference case.

In Figures 8 and 9 we see that by feeding back the base joint disturbance to the forward drive wheels (i.e. the drive wheels associated with the tipover axis) we are able to recover a stable posture while maintaining system stability throughout the recovery motion execution.

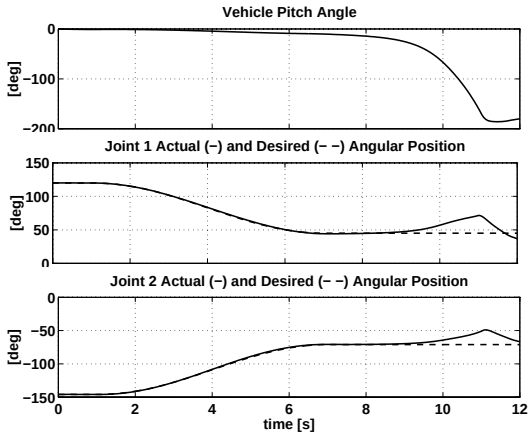

Fig. 4: **Configuration variables for unstabilized case.**

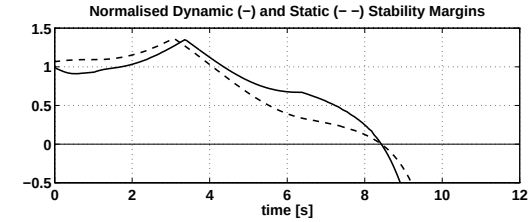

Fig. 5: **Stability margin for unstabilized case.**

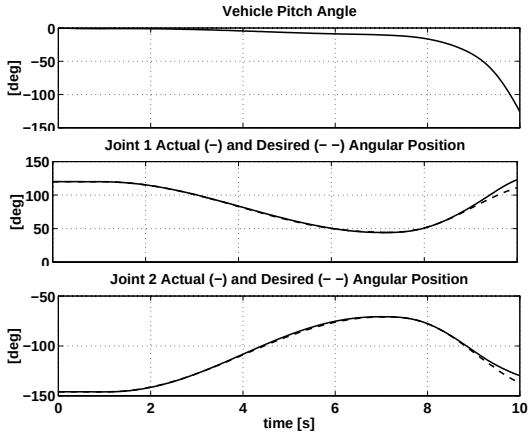

Fig. 6: **Config. variables for arm retraction only case.**

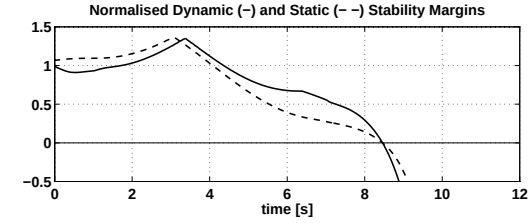

Fig. 7: **Stability margin for arm retraction only case.**

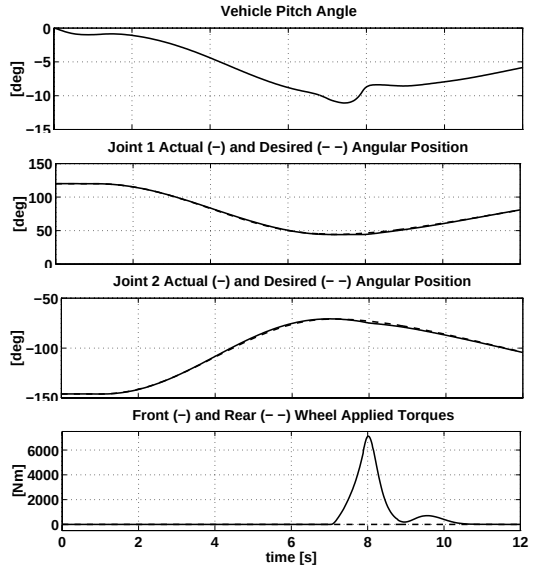

Fig. 8: **Configuration variables for fully stabilized recovery case.**

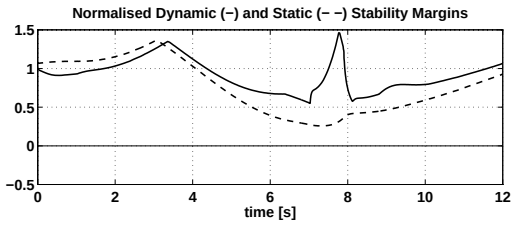

Fig. 9: **Stability margin for fully stabilized recovery case.**

5 Conclusions

This work presented an algorithm for automatic tipover *prediction* and *prevention* for mobile manipulators.

Two distinct types of tipover instability were identified: static tipover instabilities (where inertial loads are *stabilizing* the vehicle base), and dynamic tipover instabilities (where inertial loads are *destabilizing* the vehicle base.) It was found that performance of an automatic tipover prevention scheme is improved by tracking the stability margin associated with both of these measures.

A tipover *prediction* technique was presented which made use of the dynamic Force–Angle measure of the tipover stability margin [10] and a newly introduced static version of the latter. It was shown that by estimating the gradient of the stability margin measures, static and dynamic time-until-tipover predictions can be computed and used to trigger a tipover prevention response. A tipover prevention response triggering algorithm was presented which limits automatic responses to those cases where the tipover predictions are persistent.

Finally, a tipover *prevention* technique was presented which uses the platform wheels, tracks or legs to compensate for destabilizing moments at the manipulator base when the latter is retracted to regain a statically stable pose. Performance of the proposed technique was demonstrated using a forestry vehicle simulation of an unstable pick-and-place task.

Future work will examine the effectiveness of the proposed tipover prevention technique for various mobile manipulator architectures performing a variety of tasks.

Acknowledgements

The support of this work by the IRIS–2 Centres of Excellence (ISDE-4) is gratefully acknowledged.

References

[1] I. S. Jones and M. B. Penny, "Engineering parameters related to rollover frequency," *SAE Trans.*, no. 900104, 1990.

[2] W. Buchele and L. Xie, "Computer analysis of the lateral stability of agricultural tractors," in *Amer. Society of Agricultural Eng. Winter Meeting*, no. 901589, 1990.

[3] S. Dubowsky and E. E. Vance, "Planning mobile manipulator motions considering vehicle dynamic stability constraints," in *IEEE Int. Conf. on Robotics and Automation*, (Scottsdale, AZ), pp. 1271–1276, May 1989.

[4] Z. Shiller and Y.-R. Gwo, "Dynamic motion planning of autonomous vehicles," *IEEE Trans. on Robotics and Automation*, vol. 7, pp. 241–249, Apr. 1991.

[5] R. B. McGhee and G. I. Iswandhi, "Adaptive locomotion of a multilegged robot over rough terrain," *IEEE Trans. on Systems, Man, and Cybernetics*, vol. SMC-9, no. 4, pp. 176–182, 1979.

[6] S. M. Song and K. Waldron, *Machines that Walk.* Cambridge, MA: MIT Press, 1989.

[7] S. Sugano, Q. Huang, and I. Kato, "Stability criteria in controlling mobile robotic systems," in *IEEE/RSJ Int. Workshop on Intelligent Robots and Systems*, (Yokohama, Japan), pp. 832–838, July 1993.

[8] J. K. Davidson and G. Schweitzer, "A mechanics-based computer algorithm for displaying the margin of static stability in four-legged vehicles," *Trans. ASME J. Mechanical Design*, vol. 112, pp. 480–487, Dec. 1990.

[9] D. A. Messuri and C. A. Klein, "Automatic body regulation for maintaining stability of a legged vehicle during rough-terrain locomotion," *IEEE J. Robotics and Automation*, vol. RA-1, pp. 132–141, Sept. 1985.

[10] E. G. Papadopoulos and D. A. Rey, "A new measure of tipover stability margin for mobile manipulators," in *IEEE Int. Conf. on Robotics and Automation*, (Minneapolis, MN), pp. 3111–3116, April 1996.

[11] D. Karnopp, "Computer simulation of slip-stick friction in mechanical dynamic systems," *Trans. ASME J. Dynamic Systems, Measurement, and Control*, vol. 107, pp. 100–103, 1985.